Cell Death and Differentiation (2006) 13, 2068–2078

www.nature.com/cdd

Increased apoptosis, huntingtin inclusions and altered differentiation in muscle cell cultures from Huntington's disease subjects

A Ciammola*[,1,8], J Sassone[1,8], L Alberti[2], G Meola[3], E Mancinelli[4], MA Russo[5,6], F Squitieri*[,7] and V Silani[1]

[1] Department of Neurology and Laboratory of Neuroscience, 'Dino Ferrari' Center, University of Milan Medical School, IRCCS Istituto Auxologico Italiano, Milan, Italy
[2] Unit of Metabolic Diseases and Diabetes, IRCCS Istituto Auxologico Italiano, Milan, Italy
[3] Department of Neurology, University of Milan Medical School, San Donato Hospital, San Donato, Italy
[4] Department of Biomolecular Sciences and Biotechnologies, University of Milan, Milan, Italy
[5] Department of Experimental Medicine and Pathology, University 'La Sapienza', Rome, Italy
[6] IRCCS San Raffaele La Pisana, Rome, Italy
[7] Neurogenetics Unit and Centre for Rare Diseases, IRCCS Neuromed, Pozzilli (IS), Italy
[8] These authors contributed equally to this work.
* Corresponding authors: A Ciammola, Department of Neurology and Laboratory of Neuroscience, IRCCS Istituto Auxologico Italiano, via Spagnoletto 3, 20149, Milan, Italy; Tel: +39 02-619112937; Fax: +39 02-619112937; E-mail: a.ciammola@auxologico.it or F Squitieri, Neurogenetics Unit and Centre for Rare Diseases, IRCCS Neuromed, Localita' Camerelle, 86077, Pozzilli (IS), Italy. Tel.: +39 0865 915238; Fax: +39 0865 927575; E-mail: neurogen@neuromed.it

Received 08.8.05; revised 27.3.06; accepted 11.4.06; published online 26.5.06
Edited by L Greene

Abstract

Mutated huntingtin (htt) is ubiquitously expressed in tissues of Huntington's disease (HD) patients. In the brain, the mutated protein leads to neuronal cell dysfunction and death, associated with formation of htt-positive inclusions. Given increasing evidence of abnormalities in HD skeletal muscle, we extensively analyzed primary muscle cell cultures from seven HD subjects (including two unaffected mutation carriers). Myoblasts from presymptomatic and symptomatic HD subjects showed cellular abnormalities *in vitro*, namely mitochondrial depolarization, cytochrome *c* release, increased caspase-3, -8, and -9 activities, and defective cell differentiation. Another notable feature was the formation of htt inclusions in differentiated myotubes. This study helps to advance current knowledge about the downstream effects of the htt mutation in human tissues. Further applications may include drug screening using this human cellular model.

Cell Death and Differentiation (2006) **13,** 2068–2078.
doi:10.1038/sj.cdd.4401967; published online 26 May 2006

Keywords: Huntington's disease; human muscle cell cultures; apoptosis; mitochondrial membrane potential; huntingtin inclusions

Abbreviations: HD, Huntington's disease; htt, huntingtin; DAPI, 4,6-diamidine-2-phenylindole, dihydrochloride

Introduction

Huntington's disease (HD) is a neurodegenerative disorder caused by a dominant CAG expansion mutation over 35 triplets encoding a longer polyglutamine tract in huntingtin (htt), a large protein widely expressed in nervous and non-nervous tissues including skeletal muscle.[1] In patients, progressive widespread brain atrophy,[2,3] leading to severe motor disability over time, is associated with early peripheral tissue dysfunction such as loss of body weight.[4,5] Hence, the pathological involvement of non-nervous tissues may contribute to the clinical features of HD.

In particular, accrued evidence over the past 10 years has documented skeletal muscle dysfunction in HD. Defects in muscular energy metabolism have been found in symptomatic and presymptomatic HD subjects[6,7] and mitochondrial complex deficiency associated with unspecific myopathic changes have been described in muscle biopsies from symptomatic patients.[8] Furthermore, immunohistochemical studies detected the formation of htt aggregates in human skeletal muscle.[9] Abnormal features have also been confirmed in an HD transgenic mouse model R6/2, where similar degenerative changes involved both brain and muscle fibers. Precisely, analysis of R6/2 peripheral tissues identified htt inclusions and atrophy in muscle fibers, whereas htt inclusions were absent from other peripheral tissues including skin and adipose tissue.[10] Studies in more recent years tested the hypothesis that changes in neuronal gene expression would be mirrored in skeletal muscle, showing parallel changes first in muscle and brain from R6/2,[11] then in muscle from transgenic models and HD patients.[12] These results suggest that muscle gene expression might serve as a biomarker for therapeutic trials.

Although skeletal muscle might therefore be a useful model for studying the pathogenic mechanisms underlying HD, to our knowledge no studies have investigated *in vitro* the features of primary muscle cells from patients with HD. Understanding the mutated-htt dependent mechanisms underlying human muscle cell dysfunction and death is important for two reasons. First, because it should provide new insights into the mechanisms involved in neuronal abnormalities and neurodegeneration in HD, and also because the cellular model, by disclosing pathological features, could be useful for testing therapeutic strategies and for drug screening.

In this study we therefore conducted an extensive analysis aimed at investigating cell dysfunction and death in muscle cell cultures from seven patients with HD (including two presymptomatic subjects).

Results

Htt expression and inclusions in muscle cell cultures

Normal myoblasts and HD myoblasts both displayed diffuse cytoplasmic labeling for htt, more intense in the perinuclear region. No difference was found in the intensity and pattern of htt staining between HD and control myoblasts, nor were nuclear or cytoplasmic inclusions observed (Supplementary Figure 5). Control and HD myotubes immunostained for htt more intensely than myoblasts and, notably, MAB2166 detected rounded, cytoplasmic inclusions of various sizes, only in HD myotubes. Cytoplasmic inclusions were visible in $5\pm3\%$ of myotubes from all the symptomatic and presymptomatic HD subjects, and double immunofluorescence labeling demonstrated apparent ubiquitination in a subset of htt-immunoreactive inclusions (Figure 1a–f).

Muscle cell differentiation

In all HD cell cultures we detected altered myotube formation. The fusion index was significantly lower in HD myotubes than in control cells ($47\pm2\%$ in HD *versus* $55\pm3\%$ in controls, $P<0.01$) (Figure 1g). HD myotubes also contained fewer nuclei than controls (4.6 ± 0.3 in HD *versus* 6.7 ± 0.6 in controls, $P<0.001$, Figure 1h). The distribution of nuclei also differed markedly in control and HD myotubes. About 20% of control myotubes contained more than nine nuclei, 36% from five to nine and 44% from two to four. Conversely, most HD myotubes contained from two to four nuclei and only 11% contained more than nine (Figure 1i).

Increased susceptibility to apoptosis in human HD myoblasts

At phase contrast microscopy, control myoblasts were fine, spindle-shaped, and grew in characteristically orderly arrays (Figure 2a), whereas myoblasts from HD subjects grew in a disorderly way, were irregular in shape and showed the typical features of apoptotic cell death, namely cellular fragmentation and cytoplasmic shrinkage (Figure 2b).[13] HD myoblasts also contained several cytoplasmic vacuoles, whereas control cells did not (Figure 2a and b). On day 7 in differentiation medium, both HD and control cultures contained a mixture of myoblasts and myotubes, although HD cell cultures had a lower fusion index (Figures 1g, 2c and d) and smaller myotubes than control cultures (Figures 1h and i, 2c and d). Unlike undifferentiated HD myoblasts, myotubes never displayed vacuolation.

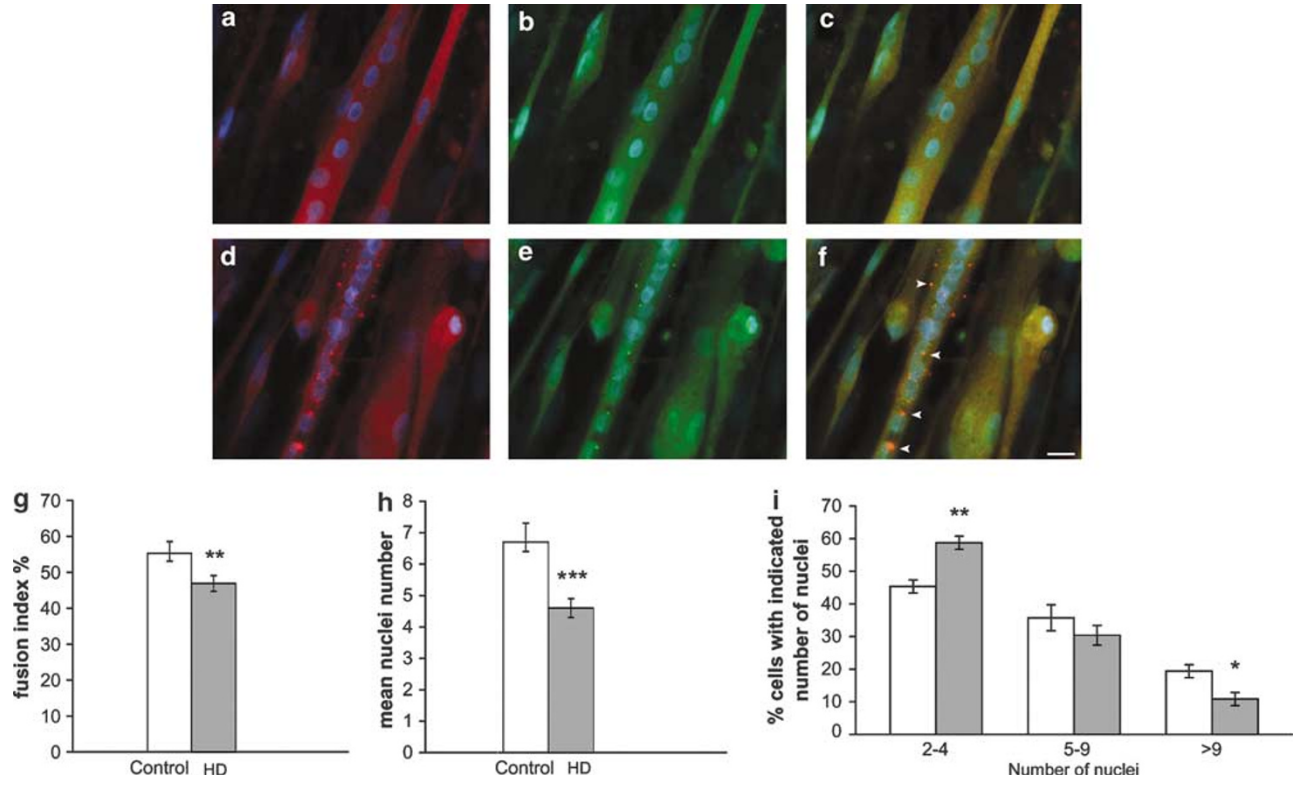

Figure 1 Immunofluorescence analysis and myotube formation in muscle cell cultures from HD and control subjects. MAB2166 immunoreactivity (red fluorescence) and ubiquitin immunoreactivity (green fluorescence) in control (**a–c**) and HD (**d–f**) myotubes. Colocalization is shown in merged images in the right panel (yellow fluorescence). HD myotubes exhibited inclusions that were immunoreactive for huntingtin and ubiquitin (arrow heads). Scale bar represents 10 μm. Quantification of myotube formation. (**g**) Fusion index and (**h**) mean nuclei number were measured for control and HD cells. (**i**) The graph shows the percentage of myotubes with two to four nuclei, five to nine nuclei, 10 or more nuclei in HD (gray columns) and control (white columns) cultures. Results are means $\pm$ S.E.M. from four experiments performed on myotubes from nine controls and seven HD subjects; $^{*}P<0.05$, $^{**}P<0.01$, $^{***}P<0.001$ *versus* control myoblasts

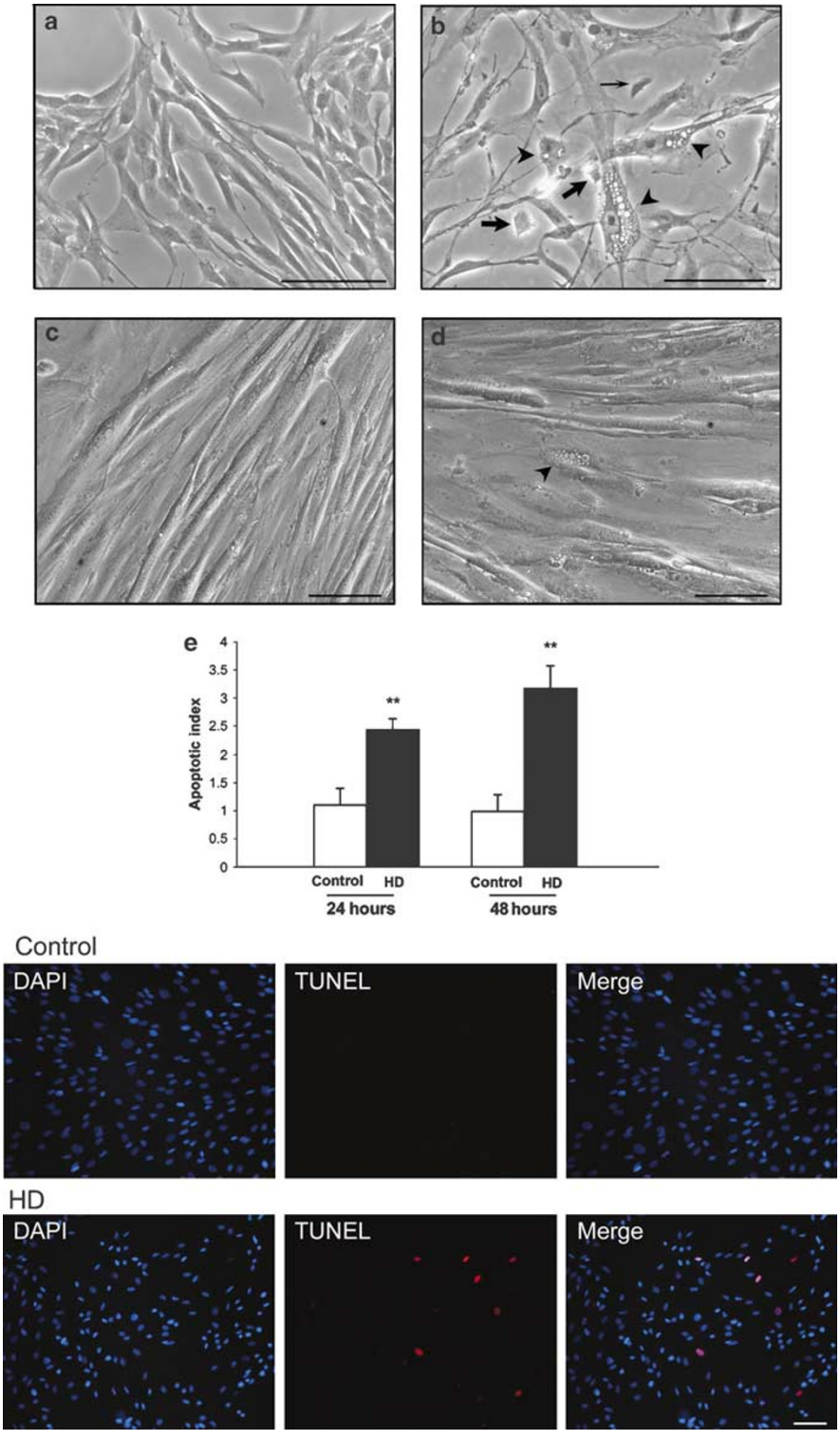

Figure 2 Analysis of morphology and apoptotic index in muscle cell cultures. Morphological characterization of control (**a**) and HD (**b**) myoblasts. Cytoplasmic shrinkage (large arrows), cellular fragmentation (small arrow) and vacuoles (arrow heads) can be detected only in myoblasts from symptomatic and asymptomatic HD subjects. Scale bars represent 50 μm. Morphology of control (**c**) and HD (**d**) myotubes at day 7 in differentiating medium. A few vacuoles were still observed in undifferentiated myoblasts (arrow head). Scale bars represent 50 μm. (**e**) *In situ* apoptotic index of control and HD myoblasts 24 and 48 h after plating. The graph represents means $+$ S.E.M. of four independent experiments performed on myoblasts from nine controls and seven HD subjects; $^{**}P < 0.01$ *versus* control myoblasts. Representative photomicrographs show TUNEL-positive nuclei in control and HD myoblasts 24 h after plating (red fluorescence)

The apoptotic index measured after plating was significantly higher in HD myoblasts than in controls, at 24 h (2.4 ± 0.2% *versus* 1.1 ± 0.3%; $P < 0.01$) and at 48 h (3.2 ± 0.3% *versus* 1.0 ± 0.3%; $P < 0.01$), (Figure 2e). As our data showed an equally high proliferative rate under normal growth conditions in control and HD myoblasts (Figure 3a), we tested viability under stressful conditions. HD myoblasts were more sensitive than control cells to all tested mitochondrial chain inhibitors. At low drug concentrations inhibition of proliferation started early and at higher drug concentrations cell numbers sharply decreased in HD myoblasts (Figure 3b–e). After cell cultures were deprived of serum, proliferation of both HD and control myoblasts began to decrease. From day 7 onwards, progressive cell death began but only in HD cell cultures (Figure 3f).

Mitochondrial membrane potential ($\Delta\Psi_m$) dissipation and cytochrome *c* release in HD myoblasts

Analysis of JC-1 fluorescence emission under normal growth conditions showed lower mitochondrial membrane potential ($\Delta\Psi_m$) in HD myoblasts than in controls (Figure 4a).

The proapoptotic factor cytochrome *c* was detected in cytosolic fractions from HD myoblasts, but not in controls (Figure 4b). An ELISA assay to quantify cytochrome *c* further confirmed that cytochrome *c* was present in significant amounts only in cytosol from HD cells (Figure 4c). Immunofluorescence analysis confirmed that in healthy myoblasts cytochrome *c* colocalized with mitochondria, whereas in HD myoblasts it showed diffuse cytoplasmic staining (Figure 4d–i).

To investigate the role of the mPTP in $\Delta\Psi_m$ dissipation induced by endogenous mutated htt in myoblasts, we analyzed $\Delta\Psi_m$ after suppressing CypD expression by RNAi. The specific CypD-RNAi produced a sharp decrease in the amount of CypD mRNA (Figure 5a and Supplementary Figure 6) and CypD protein (Figure 5b). Moreover, the CypD-deficiency strongly protected both HD and control myoblasts from Ca^{2+} induced mPTP opening (Supplementary Figure 7).[14,15] Despite protecting mPTP opening, the CypD-deficiency left the difference in $\Delta\Psi_m$, between HD and control myoblasts, under normal growth conditions, unchanged (Figure 5c).

Caspase activities in HD myoblasts

Under normal growth conditions, we observed a caspase-3-like activity, which was significantly higher in HD myoblasts than in control cells (4.4 ± 0.3 *versus* 2.7 ± 0.4 DEVDase enzymatic assay; $P < 0.001$), (Figure 6a). This finding was confirmed by Western blotting using a specific antibody against the active caspase-3 fragment (Figure 6b). Under normal growth conditions, HD myoblasts also showed, increased caspase-9-like (11.4 ± 0.5 *versus* 8.3 ± 0.5; $P < 0.001$) and caspase-8-like (8.1 ± 0.8 *versus* 5.7 ± 0.8; $P < 0.01$) activities (Figure 6c).

As caspase-3, -8 and -9 activities were increased in HD cells, we tested whether a broad-spectrum caspase inhibitor could reduce HD myoblast death. In this experiment, 100 μM ZVAD-FMK significantly reduced the apoptotic index in HD cells (apoptotic index 34 ± 9%; $P < 0.01$ after 24 h, 27 ± 8%; $P < 0.01$ after 48 h; Figure 7a).

As we had found increased vulnerability to mitochondrial complex inhibitors in HD myoblasts (Figure 3), we assessed whether such reduced viability might be dependent on caspase-3 activation. We first monitored caspase-3 activity in myoblasts treated with mitochondrial toxins and found that, although caspase-3 activity increased in both HD and control myoblasts, caspase-3 always reached higher levels in HD cells than in control cells, accounting for the previous viability assays (Figure 7b). Second, we tested whether caspase inhibition could reduce this sensitivity to mitochondrial toxins. ZVAD-FMK increased viability more strongly in HD than in control cells (Figure 7c, black column), canceling the differences between control cells and cells from HD subjects. Selective caspase-8 (IETD-FMK) and caspase-9 inhibitors (LEHD-FMK) also promoted a significant but lower survival in HD cells (Figure 7c, gray columns).

Discussion

In this *in vitro* study, we provide evidence of cell dysfunction and apoptosis in muscle cell cultures from subjects with HD. The characteristic abnormal features we detected were the formation of htt-immunoreactive inclusions, altered differentiation and apoptotic events, including mitochondrial depolarization and increased caspase activities.

An interesting finding was the *in vitro* evidence of muscle cell dysfunction and apoptosis even in the two subjects still at the presymptomatic stage of HD. Our study therefore suggests that muscle cell dysfunction may start early in life, accumulates over time and generates damage in advanced HD, along with the loss of motor and cognitive functions due to brain involvement. Our *in vitro* model based on a tissue directly obtained from HD subjects, thus expressing endogenous mutated protein in its physiological setting, could be useful for documenting pathological changes taking place *in vivo*, even during the presymptomatic stage of the disease.

The pathogenic role of htt aggregates in HD is still controversial. In agreement with data from transgenic models,[10,16] we found that inclusion bodies were selectively distributed in HD myotubes (Figure 1a–f) but not in HD myoblasts, implying that such formations may not be essential for inducing cell death.[17] The inclusion bodies we observed in *ex vivo* myotubes resemble htt-immunoreactive granular deposits, recently detected in human post-mortem HD muscles.[9]

Our findings provide evidence favoring increased apoptotic death in HD myoblasts (Figure 2), with reduced viability under stressful conditions (Figure 3b–f). As myoblasts are essential, *in vivo*, for normal growth, repair, and maintenance of adult skeletal muscle bulk,[18] an increased rate of cell death associated with impaired myotube formation may contribute to the progressive weight loss observed in patients with HD.[5] The increased apoptosis and muscle cell dysfunction are consistent with the severe muscular atrophy detected in transgenic HD mice[10] and accord with nonspecific myopathic

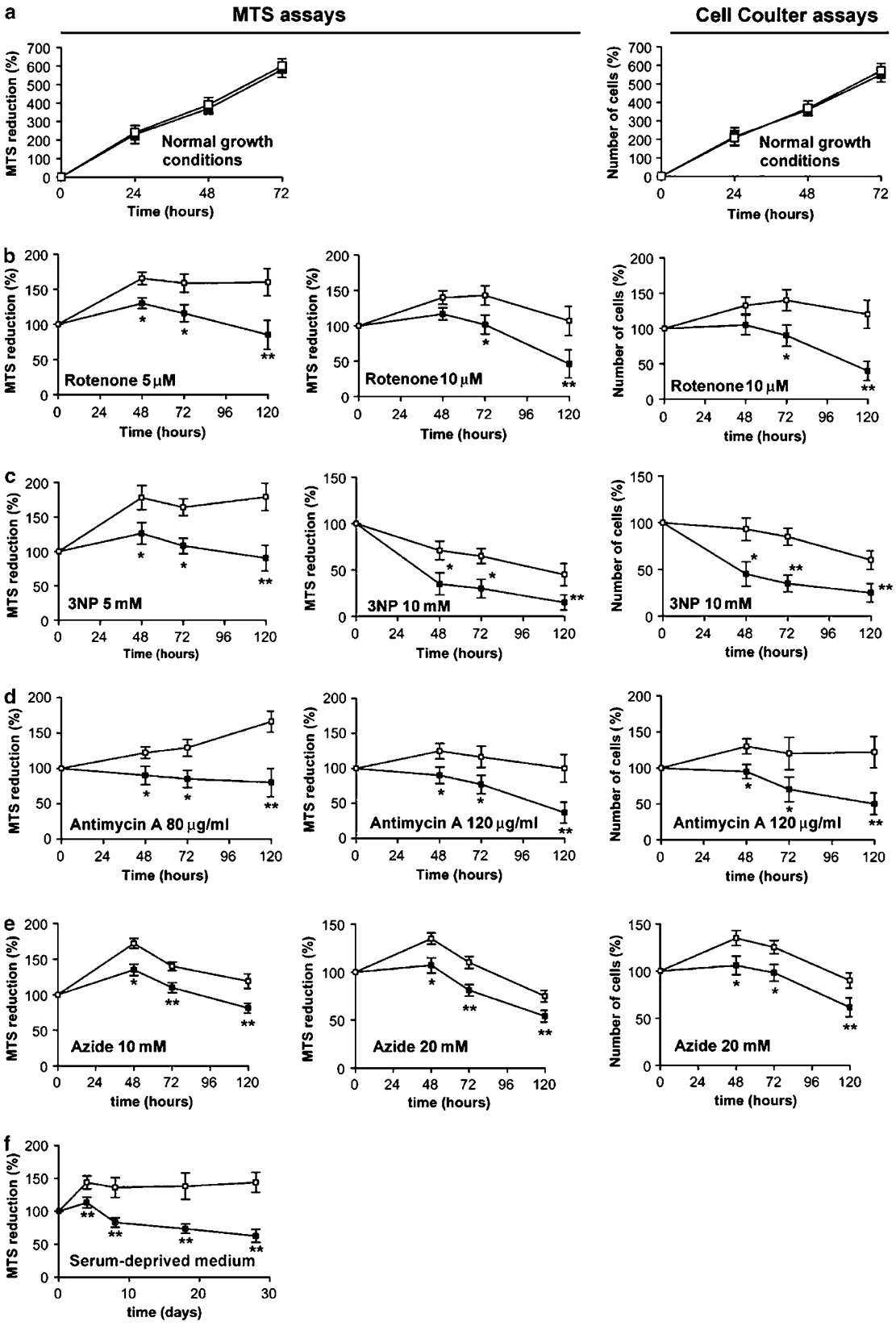

Figure 3 Analysis of myoblast survival. HD (filled squares) and control (open squares) myoblast survival. The assays were performed under (**a**) normal growth conditions, after treatment with (**b**) 5 and 10 μM rotenone, (**c**) 5 and 10 mM 3NP, (**d**) 80 and 120 μg/ml antimycin A, and (**e**) 10 and 20 mM azide and in (**f**) serum-deprived medium. The graphs show the mean $\pm$ S.E.M. of MTS assays (five independent experiments) and Coulter counter assays (three independent experiments) performed on myoblasts from nine controls and seven HD subjects. $^{*}P<0.05$, $^{**}P<0.01$ *versus* control myoblasts

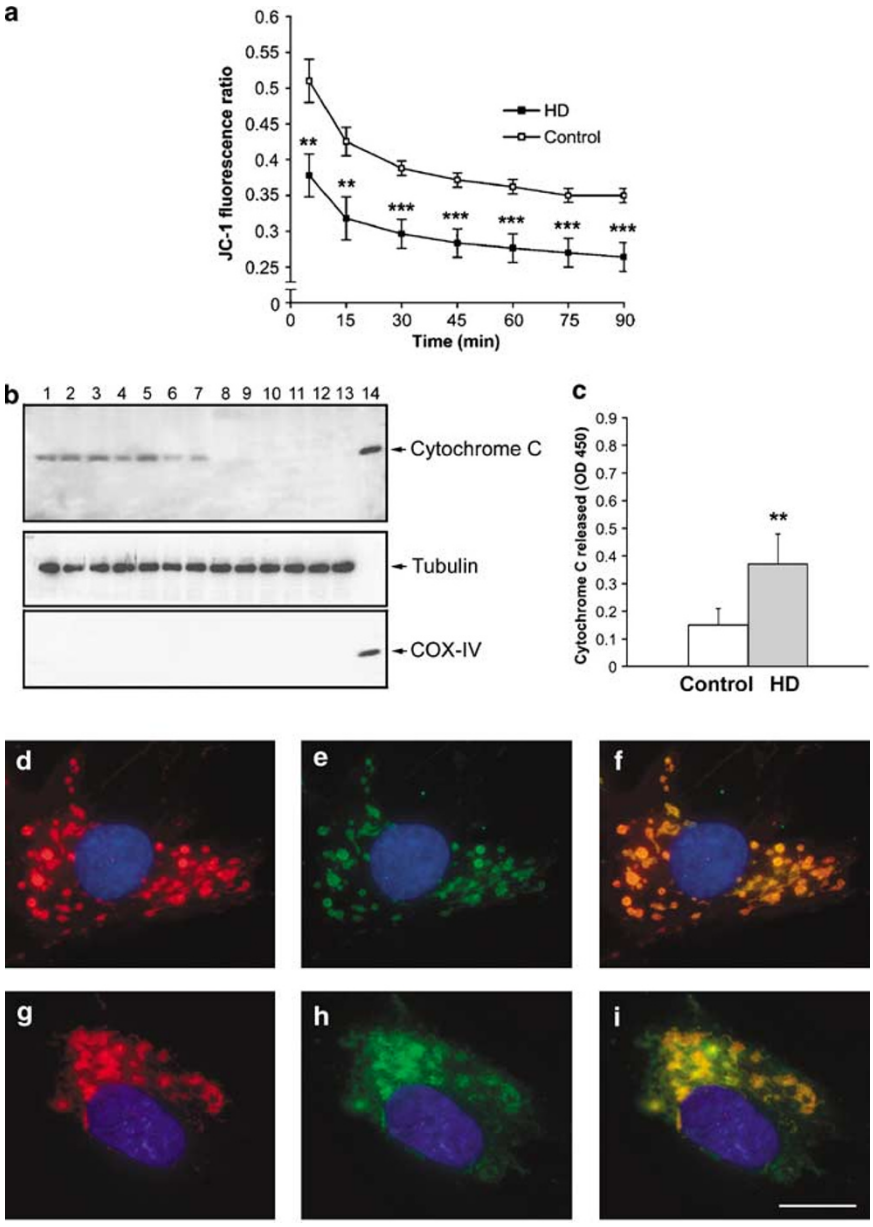

Figure 4 Analysis of $\Delta\Psi_m$ and cytochrome *c* release in myoblasts. (**a**) JC-1 fluorescence ratio (red/green emission) of HD and control myoblasts. The signal was followed over an extended period of time to validate the stability of the probe once incorporated in the living cells. Values represent the mean $\pm$ S.E.M. from five independent experiments performed on myoblasts from nine controls and seven HD subjects; $^{**}P<0.01$, $^{***}P<0.001$ *versus* control myoblasts. (**b**) Immunoblot of cytosolic fractions from HD (lanes 1–7) and control (lanes 8–13) myoblasts. Cells were homogenized and subjected to the preparation of cytosolic fractions as described in Materials and Methods. Lane 14 was a purified mitochondrial fraction. Membrane was stripped and reprobed with tubulin and cytochrome oxidase IV (COX-IV) antibodies. Tubulin was used to verify equal protein loading and COX-IV was used as a control for the purity of the cytosolic fractions. (**c**) The graph represents the cytochrome *c* released in the cytosol of HD and control myoblasts quantitatively examined using an ELISA assay ($^{**}P<0.01$ compared to control). Results are expressed as mean $\pm$ S.E.M. from five independent experiments performed on myoblasts from nine controls and seven HD subjects. Representative photomicrographs show MitoTrackerRed (red fluorescence) and cytochrome *c* immunoreactivity (green fluorescence) in control (**d**–**f**) and HD (**g**–**i**) myoblasts. Colocalization is shown in merged images on the right panel (yellow fluorescence). Scale bar represents 10 μm

changes reported by morphological analyses of human HD skeletal muscle.[8]

Previous reports have described altered mitochondrial oxidative metabolism in brain and peripheral tissues of HD subjects[6–9,19] and increased mitochondrial depolarization after stress conditions in both fibroblasts and lymphoblasts from HD subjects.[20,21] In our cell model, we observed mitochondrial $\Delta\Psi_m$ dissipation and cytochrome *c* release even under normal growth conditions. Muscle cells may therefore be far more vulnerable to mutated htt than other cellular models such as HD lymphoblasts or fibroblasts. If so, muscle cells could be a useful new human peripheral cell model for exploring the pathogenic mechanisms in HD.

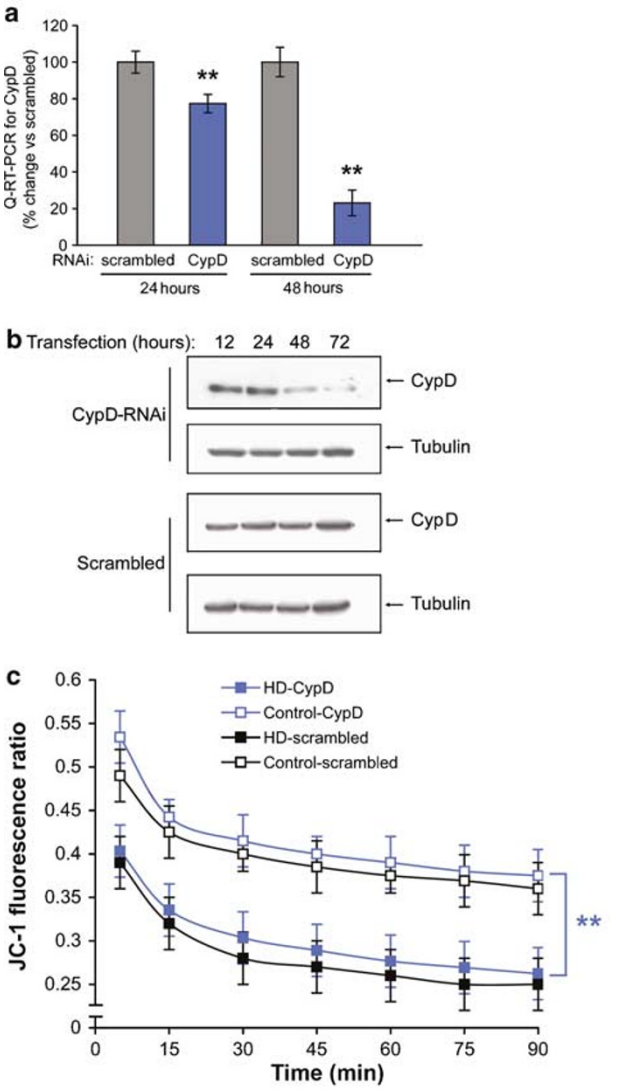

Figure 5 Effect of RNAi for CypD on $\Delta\Psi_m$. (**a**) RNAi-mediated depletion of CypD mRNA was confirmed by real-time reverse transcriptase-polymerase chain reaction (RT-PCR). The graph represents the mean ± S.D. of two independent experiments performed on myoblasts from nine controls and seven HD subjects; $^{**}P<0.01$ *versus* scrambled. (**b**) Representative immunoblot showing CypD protein depletion at 48 and 72 h after transfection of CypD-RNAi. CypD was quantified by immunoblotting on two different protein extractions from nine controls and seven HD myoblasts. (**c**) Measurements of JC-1 fluorescence ratio in HD and control CypD-deficient myoblasts at 72 h after transfection (blue lines). The figure also shows JC-1 fluorescence ratios in scrambled myoblasts (black lines); values represent the mean ± S.D. from two independent experiments performed on myoblasts from nine controls and seven HD subjects. Statistical comparisons of CypD-deficient HD myoblasts *versus* CypD-deficient control myoblasts were performed using ANOVA followed by Tukey test, $^{**}P<0.01$

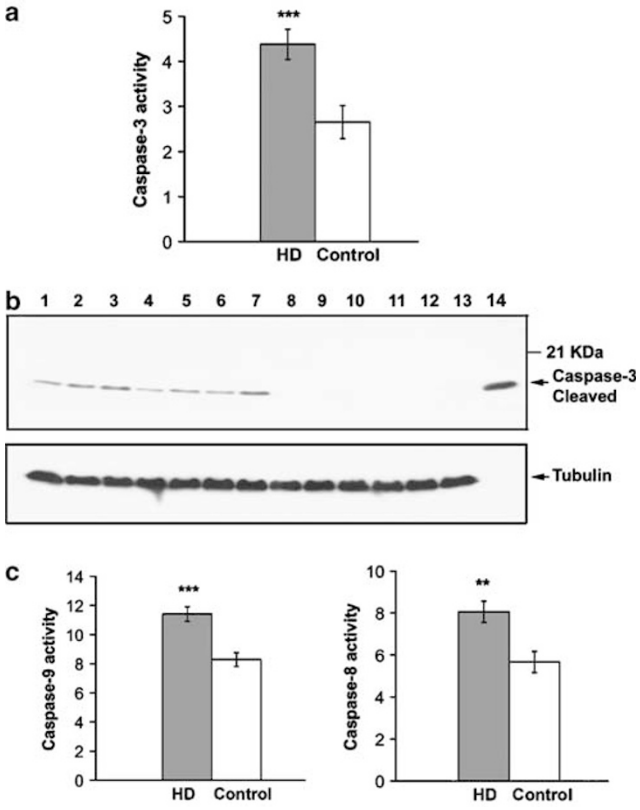

Figure 6 Caspase activities in myoblasts from HD and normal subjects. (**a**) Caspase 3-like activity in HD and control myoblasts. (**b**) Lysates from HD (lanes 1–7) and control (lanes 8–13) myoblasts were subjected to Western blot analysis with antibody for active caspase-3. Lane 14 represents a positive control (human caspase-3 active recombinant). To verify equal protein loading on each lane, membranes were stripped and reprobed for tubulin. The figure shows a representative immunoblot of four independent experiments. (**c**) Caspase 9-like and caspase 8-like activity in HD and control myoblasts. Caspase activities are expressed as specific enzymatic activity (pmol of pNA liberated/h/μg protein). Values represent the mean ± S.E.M. from five independent experiments; $^{**}P<0.01$, $^{***}P<0.001$ *versus* control myoblasts

The results of our RNAi experiments suggest that $\Delta\Psi_m$ dissipation induced by endogenous mutated htt may depend on factors other than single mPTP opening (Figures 5). Coherently with our findings, Bcl-2 family members, whose alterations have been reported in a mouse model of HD,[22] may promote cytochrome *c* release independently from mPTP opening.[14] Our data therefore strengthen the hypothesis that intrinsic mitochondrial pathways,[23] such as the cascade of toxic events associated with alterations in Bcl-2 family members, may contribute to the pathogenesis of HD and merit further analysis.

Differently from other models such as lymphoblastoid cell lines, we found increased caspase-3 activity at baseline, in unstimulated HD cells. A possible explanation is that in lymphoblasts, immortalization by a virus may significantly influence the cell proliferation rate and apoptotic cell death.[24] Although baseline caspase-3 activity is important for normal cell survival in muscle,[25] in our muscle cell model, caspase-3 activity differed significantly in cells expressing mutated htt and control cells (Figure 6a and b).

Coherently with previous reports indicating a role of caspase-8 and -9 in HD,[22,26,27] we herein describe activation of these two proteases in HD myoblasts (Figure 6c). Both caspase initiators may contribute to the pathogenic cascade of events leading to caspase-3 activation and finally to apoptosis. When we exposed HD myoblasts to a broad-spectrum caspase inhibitor the apoptotic index decreased (Figure 7a). Notably, in the presence of caspase inhibitors, the

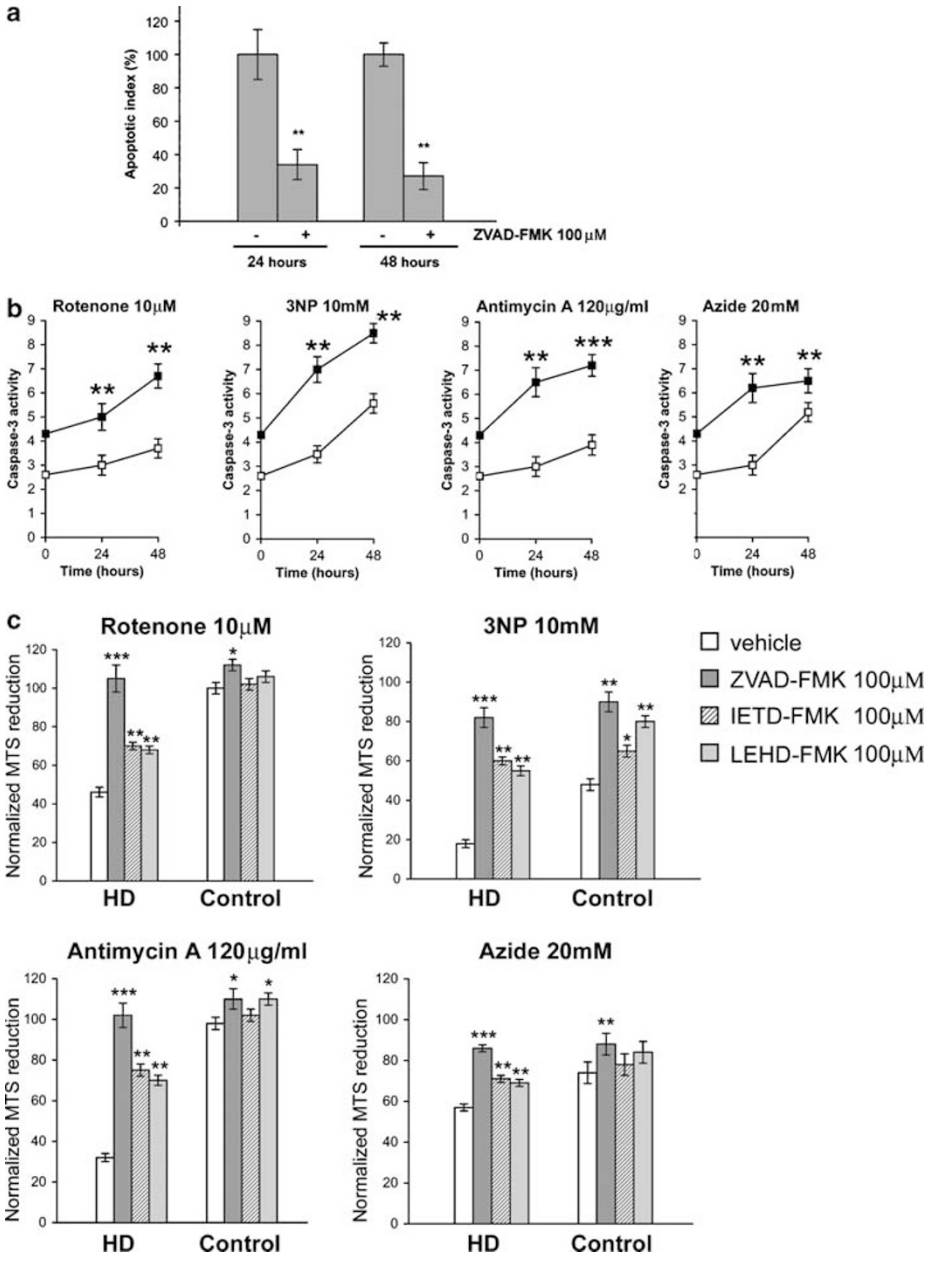

Figure 7 Effect of cell-permeable caspase inhibitors on HD myoblasts. (**a**) HD myoblasts were exposed to ZVAD-FMK for 24 and 48 h and the apoptotic index was analyzed using the TUNEL assay. The graph represents means ± S.E.M. of four independent experiments performed on myoblasts from nine controls and seven HD subjects (data were normalized and compared with untreated cultures; $^{**}P<0.01$). (**b**) Caspase-3 activity was measured 24 and 48 h after mitochondrial toxin exposure in HD (filled squares) and control (open squares) myoblasts. The graphs represent means ± S.D. from two independent experiments performed on myoblasts from nine controls and seven HD subjects.$^{**}P<0.01$ and $^{***}P<0.001$ *versus* control myoblasts. (**c**) Caspase inhibition partially prevented cell death produced by mitochondrial toxins. HD and control myoblasts were exposed to mitochondrial complex inhibitors with or without addition of caspase inhibitors, and cell survival was analyzed 120 h later using the MTS assay. Data are presented as mean ± S.E.M. from three independent experiments performed on myoblasts from nine controls and seven HD subjects; Data were normalized to MTS reduction before toxin exposure; $^{*}P<0.05$, $^{**}P<0.01$, $^{***}P<0.001$ *versus* toxin alone (vehicle-treated culture) within the same experiment

difference in viability between control and HD myoblasts under stressful conditions substantially diminished (Figure 7c), suggesting that the higher susceptibility of HD myoblasts to mitochondrial toxins is a caspase-mediated event. These findings indicate that apoptosis plays a key role in the death of HD myoblasts, even if they leave open other molecular mechanisms of cell death. For instance, a distinctive finding was the large number of cytoplasmic vacuoles detected in HD myoblasts (Figure 2a and b). This feature may be compatible with autophagic cell death, previously described in HD[28] and recently highlighted in HD lymphoblasts with large expansions[29] and homozygous CAG mutations.[30] This and other ultrastructural features will need further clarification. As the size of CAG expansions differed

little among samples, we failed to observe any dependence of cell abnormalities on subjects' genotype and phenotype (Supplementary Table 1).

Our results corroborate the hypothesis that mutated htt, ubiquitously expressed in nervous and non-nervous system,[1] also damages tissues outside the brain.[9,20,29–32] By applying these new findings in human HD muscle cells we may be able to clarify the pathogenic mechanisms induced by endogenous mutated htt and to test new therapeutic strategies *in vitro*.

Materials and Methods

Subjects and muscle biopsies

Genetic testing was performed on blood lymphocyte DNA, and the CAG trinucleotide repeat length was assessed as previously described.[33] Two unaffected mutation carriers underwent the predictive testing program according to the published protocol.[34] Demographic and clinical characteristics of the subjects are summarized in the Supplementary Table 1. Biopsy specimens were obtained from the upper limbs of seven patients with HD (mean age 44 ± 11 years) and nine healthy controls (mean age 42 ± 8 years) and processed for primary muscle cell cultures. The age difference in years between the two groups was not statistically significant ($P > 0.05$, *t*-test). The study was conducted after ethical approval of the local Bioethics Committee, and informed consent for genetic testing (molecular confirmation and predictive testing) and muscle biopsy was obtained from all subjects.

Muscle cell cultures

Myoblasts were derived in accordance with Blau and Webster[35] and grown in HAM's F10 medium (Sigma, St Louis, MO, USA) supplemented with 15% fetal bovine serum (Gibco/Invitrogen, San Diego, CA, USA), 0.5 mg/ml bovine serum albumin, 10 ng/ml epidermal growth factor, 4 ng/ml insulin, 0.39 μg/ml dexamethasone, 100 U/ml penicillin, and 0.1 mg/ml streptomycin. Cultures were stained by immunocytochemistry using antibodies to desmin (Chemicon, Temecula, CA; Calbiochem/Oncogene Research Products, Cambridge, MA, USA), a protein expressed only in myogenic cells.[36] Myogenic purity, calculated as the proportion of cells expressing desmin, exceeded 98% in all cultures (Supplementary Figure 1). All experiments involved cell cultures at identical passages and data were obtained from experiments repeated in cultures at the second, third, and fourth passage.

To confirm further the myogenicity of the cultured cells, we observed the fusion process which forms multinucleate myotubes after 7 days in differentiating medium (Dulbecco's modified Eagle's medium containing 10 μg/ml insulin and 5% fetal bovine serum) (Supplementary Figure 1). To check the ability of HD myoblasts to fuse and differentiate into multinucleated myotubes, we evaluated the fusion index calculated as the ratio of nuclei in myotubes to the total number of nuclei, the mean number of nuclei per myotube and the number of myotubes according to the number of nuclei per cell (2–4, 5–9, >9 nuclei).[37] At 7 days in the differentiating medium, we analyzed 10 fields from each of four separate cell cultures from each HD and control subject.

Immunofluorescence

Htt localization in myoblasts was investigated by immunofluorescence with antibodies (Chemicon) recognizing the N-terminal (MAB2166) and C-terminal (MAB2168) htt domains. Immunofluorescence on myotubes was performed with MAB2166 and anti-ubiquitin antibodies (Chemicon) 15 days after the addition of differentiation medium. Cell monolayers were fixed in 4% paraformaldehyde, permeabilized with 0.3% Triton X-100, thoroughly washed, and then blocked with 10% normal goat serum. Cells were incubated first with primary antibody overnight at 4°C then with the appropriate secondary antibody for 1 h. For analysis of cytochrome *c* localization, myoblasts were labeled with 500 nM MitoTrackerRed (Molecular Probes) for 30 min at 37°C, and then incubated with antibody against cytochrome *c* (Sigma). Anti-mouse and anti-rabbit Cy3- and Cy2-conjugated antibodies were supplied by Jackson ImmunoResearch (West Grove, PA, USA). Samples were observed under a Leica DMIR2 microscope, and digital images assembled using Imaging Software LeicaFW4000.

In situ nick end-labeling (TUNEL) assay

Myoblasts were assayed by TUNEL with the cell death detection kit, TMR red (Roche Diagnostics, Grenzach-Wyhlen, Germany) according to the manufacturer's instructions. The apoptotic index was expressed as a percentage of TUNEL-positive nuclei on all the nuclei, stained with 4,6-diamidine-2-phenylindole, dihydrochloride (DAPI).

Cell viability

Cell viability was assessed by Coulter Counter and MTS (3-(4,5-dimethylthiazol-2-yl)-5-(3-carboxymethoxyphenyl)-2-(4-sulfophenyl)-2*H*-tetrazolium) assays under the effect of four different mitochondrial toxins: rotenone, 3-nitropropionic acid (3NP), antimycin A, and azide (selective inhibitors, respectively, for complexes I, II, III, and IV). MTS was assessed by Cell Titer $96AQ_{ueous}$ Cell Proliferation assay (Promega, Southampton, UK) according to the manufacturer's protocol. Coulter Counter assays were performed with a Coulter Counter (Z2 Coulter Counter, Beckman-Coulter, Fullerton CA, USA).

Evaluation of $\Delta\Psi_m$

The dye JC-1 (Molecular Probes) was added directly to the cell culture medium (5 μM final concentration) and incubated for 30 min. The cells were washed once with PBS and then incubated with fresh medium. The fluorescence intensity was monitored with a fluorescence plate reader (Ascent FL Thermo Labsystems), using two excitation and emission filters 485/530 and 530/590 and the signal was followed over an extended period of time to validate the stability of the probe, once incorporated into the living cells. The ratio of red/green fluorescence was an indication of $\Delta\Psi_m$. To validate the method we monitored myoblast depolarization by different concentrations of a mitochondrial uncoupler (2,4-Dinitrophenol) and a mitochondrial complex IV inhibitor (Azide) (Supplementary Figure 2).

As mitochondrial permeability transition pore (mPTP) opening is characteristically induced by high-calcium levels[38] we evaluated the time course of $\Delta\Psi_m$, in permeabilized cells, in response to different Ca^{2+} concentrations (Supplementary Figure 3). The cells were plated in 96-well plates (10 000 cells/well) in complete medium (200 μl/well). After 18 h, the dye JC-1 was added to each well (5 μM final concentration) and incubated for 30 min. Cells were washed twice with Ca^{2+}-free balanced salt solution (pH 7.4 containing 2.9 mM KH_2PO_4, 180 mM NaCl, 38 mM Na_2H-$PO_4 \cdot 7H_2O$) and then permeabilized with 0.002% digitonin in 200 μl/well permeabilization buffer (120 mM KCl, 10 mM NaCl, 2 mM KH_2PO_4, 10 mM HEPES, 5 mM Na^+ succinate, 1 mM $MgCl_2$, 0.1 mM EGTA) for 3 min.[39,40] Permeabilized cells were then washed twice with permeabilization buffer

and kept in EGTA-free permeabilization buffer. The JC-1 fluorescence ratio was monitored for 40 min.

Cytochrome *c* assay

Cytochrome *c* was assayed in cytosolic fraction with the cytochrome *c* ELISA kit (Chemicon).

RNA interference against cyclophilin D

The following duplexed RNA oligonucleotides (Stealth RNA interference (RNAi)) were synthesized by Invitrogen (sense RNA sequence): cyclophilin D (CypD), 5′-GCAGAAUUGCUGAAAGUCAAACAAA-3′; scrambled, 5′-GCAUAGUUCAGAAUGACAACAGAAA-3′.

Cells were transfected with Lipofectamine 2000 (Invitrogen, Carlsbad, CA, USA) according to the manufacturer's protocol. $\Delta\Psi_m$ levels were measured 72 h after transfection. The transfection efficiency of each duplex RNAi ($>80\%$) was confirmed with Block-iT Fluorescent Oligo (Invitrogen) and transfected cells were counted with a FACSCalibur flow cytometer (Becton Dickinson Biosciences, San Jose, CA, USA) (Supplementary Figure 4). Control and HD CypD-deficient myoblasts both proliferated at a normal rate apparently without phenotypic differences compared with scrambled-transfected or untransfected cells (data not shown).

CypD mRNA expression

Total RNA from primary cultures was extracted using TRIzol (Invitrogen) according to the manufacturer's protocol. Total RNA (1 μg) was reverse transcribed using SuperScript II (Invitrogen). A real-time polymerase chain reaction (PCR) method was used to quantify CypD mRNA. For each sample, 10 ng of template was amplified in duplicate in PCR reactions on an ABI PRISM 7700 machine using Assay-on-Demand Gene Expression Products (Applied Biosystems, Foster City, California, USA). CypD mRNA and the housekeeping gene (HPRT) were labeled with FAM. Data were analyzed with the SDS 2.1 software. The relative amount of CypD mRNA was normalized to the amount of HPRT transcript in the same cDNA and data are expressed as $2^{-\Delta CT}$.

DEVDase, LEHDase, and IETDase activity

Caspase activities were monitored by a colorimetric kit (Chemicon) according to the manufacturer's protocol. Lysates were incubated at 37°C for 4 h in caspase assay buffer supplemented with specific colorimetric substrates (DEVD-pNA for caspase-3, IETD-pNA for caspase-8, and LEHD-pNA for caspase-9). Caspase activities were calculated as pmol *p*-nitroanilide liberated/h/μg protein.

Sample preparation and Western blotting

Muscle cells were rinsed with cold PBS and harvested by scraping and centrifugation, then lysed on ice for 15 min in a buffer containing 20 mM TRIS pH 7.5, 150 mM NaCl, 1 mM EDTA, 1 mM EGTA, 1% Triton X-100, and complete protease inhibitors (Roche). Equal amounts of protein were separated on polyacrylamide gel electrophoresis, transferred to polyvinylidene fluoride membranes (Amersham Pharmacia Biotech, Little Chalfont, UK), incubated in blocking buffer for 1 h (5% low fat milk in TBST, 50 mM TRIS pH 7.6, 0.15 M NaCl, 0.05% Tween), and probed overnight with the primary antibody in TBST. Antibodies for cytochrome *c*, CypD and for active caspase-3 fragments were obtained from BD Biosciences Pharmingen. Recombinant caspase-3 was obtained from Sigma. Protein bands were visualized with horseradish peroxidase-conjugated secondary antibodies and enhanced chemiluminescence (Amersham).

Statistical analysis

Unless otherwise stated all data are expressed as means $\pm$ S.E.M. Data were subjected to a normality test. As data showed a normal distribution, we used a parametric analysis of variance (ANOVA), followed by Tukey test to detect significant differences among groups. Statistical significance was set at $P<0.05$.

Acknowledgements

We would like to thank the patients and their families (Associazione Italiana Corea di Huntington-Neuromed; Associazione 'Mauro Emolo' O.N.L.U.S), without whose generous support none of this research would have been possible, the Italian Health Ministry (FS, Progetto Finalizzato 2003, Progetto Cofin 2006 and Siena Biotech; AC and FS, Malattie Neurodegenerative ex art. 56 legge finanziaria 2004) and the European Huntington Disease Network (FS). We thank Dr. Maria Orietta Borghi who performed flow cytometry analysis.

References

1. Sharp AH, Loev SJ, Schilling G, Li SH, Li XJ, Bao J, Wagster MV, Kotzuk JA, Steiner JP, Lo A, Hedreen J, Sisodia S, Snyder SH, Dawson TM, Ryugo DK and Ross CA (1995) Widespread expression of Huntington's disease gene (IT15) protein product. Neuron 14: 1065–1074.
2. Rosas HD, Koroshetz WJ, Chen YI, Skeuse C, Vangel M, Cudkowicz ME, Caplan K, Marek K, Seidman LJ, Makris N, Jenkins BG and Goldstein JM (2003) Evidence for more widespread cerebral pathology in early HD: an MRI-based morphometric analysis. Neurology 60: 1615–1620.
3. Fennema-Notestine C, Archibald SL, Jacobson MW, Corey-Bloom J, Paulsen JS, Peavy GM, Gamst AC, Hamilton JM, Salmon DP and Jemigan TL (2004) *In vivo* evidence of cerebellar atrophy and cerebral white matter loss in Huntington disease. Neurology 63: 989–995.
4. Hamilton JM, Wolfson T, Peavy GM, Jacobson MW, Corey-Bloom J and Huntington Study Group (2004) Rate and correlates of weight change in Huntington's disease. J. Neurol. Neurosurg. Psychiatry 75: 209–212.
5. Djousse L, Knowlton B, Cupples LA, Marder K, Shoulson I and Myers RH (2002) Weight loss in early stage of Huntington's disease. Neurology 59: 1325–1330.
6. Koroshetz WJ, Jenkins BG, Rosen BR and Beal MF (1997) Energy metabolism defects in Huntington's disease and effects of coenzyme Q10. Ann. Neurol. 41: 160–165.
7. Lodi R, Schapira AH, Manners D, Styles P, Wood NW, Taylor DJ and Warner TT (2000) Abnormal *in vivo* skeletal muscle energy metabolism in Huntington's disease and dentatorubropallidoluysian atrophy. Ann. Neurol. 48: 72–76.
8. Arenas J, Campos Y, Ribacoba R, Martin MA, Rubio JC, Ablanedo P and Cabello A (1998) Complex I defect in muscle from patients with Huntington's disease. Ann. Neurol. 43: 397–400.
9. Saft C, Zange J, Andrich J, Muller K, Lindenberg K, Landwehrmeyer B, Vorgerd M, Kraus PH, Przuntek H and Schols L (2005) Mitochondrial impairment in patients and asymptomatic mutation carriers of Huntington's disease. Mov. Disord. 20: 674–679.
10. Sathasivam K, Hobbs C, Turmaine M, Mangiarini L, Mahal A, Bertaux F, Wanker EE, Doherty P, Davies SW and Bates GP (1999) Formation of polyglutamine inclusions in non-CNS tissue. Hum. Mol. Genet. 8: 813–822.
11. Luthi-Carter R, Hanson SA, Strand AD, Bergstrom DA, Chun W, Peters NL, Woods AM, Chan EY, Kooperberg C, Kraine D, Young AB, Tapscott SJ and Olson JM (2002) Dysregulation of gene expression in the R6/2 model of

polyglutamine disease: parallel changes in muscle and brain. Hum. Mol. Genet. 11: 1911–1926.
12. Strand AD, Aragaki AK, Shaw D, Bird T, Holton J, Turner C, Tapscott SJ, Tabrizi SJ, Schapira AH, Kooperberg C and Olson JM (2005) Gene expression in Huntington's disease skeletal muscle: a potential biomarker. Hum. Mol. Genet. 14: 1863–1876.
13. Kerr JF, Wyllie AH and Currie AR (1972) Apoptosis: a basic biological phenomenon with wide-ranging implications in tissue kinetics. Br. J. Cancer 26: 239–257.
14. Baines CP, Kaiser RA, Purcell NH, Blair NS, Osinska H, Hambleton MA, Brunskill EW, Sayen MR, Gottlieb RA, Dorn GW, Robbins J and Molkentin JD (2005) Loss of cyclophilin D reveals a critical role for mitochondrial permeability transition in cell death. Nature 434: 658–662.
15. Nakagawa T, Shimizu S, Watanabe T, Yamaguchi O, Otsu K, Yamagata H, Inohara H, Kubo T and Tsujimoto Y (2005) Cyclophilin D-dependent mitochondrial permeability transition regulates some necrotic but not apoptotic cell death. Nature 434: 652–658.
16. Orth M, Cooper JM, Bates GP and Schapira AH (2003) Inclusion formation in Huntington's disease R6/2 mouse muscle cultures. J. Neurochem. 87: 1–6.
17. Arrasate M, Mitra S, Schweitzer ES, Segal MR and Finkbeiner S (2004) Inclusion body formation reduces levels of mutant huntingtin and the risk of neuronal death. Nature 431: 805–810.
18. Chargè SBP and Rudnicki MA (2004) Cellular and molecular regulation of muscle *regeneration.* Physiol. Rev. 84: 209–238.
19. Gu M, Gash MT, Mann VM, Javoy-Agid F, Cooper JM and Schapira AH (1996) Mitochondrial defect in Huntington's disease caudate nucleus. Ann. Neurol. 39: 385–389.
20. Sawa A, Wiegand GW, Cooper J, Margolis RL, Sharp AH, Lawler Jr JF, Greenamyre JT, Snyder SH and Ross CA (1999) Increased apoptosis of Huntington disease lymphoblasts associated with repeat length-dependent mitochondrial depolarization. Nat. Med. 5: 1194–1198.
21. Peng T-I, Obertone TS and Greenamyre JT (1998) Altered calcium responses in Huntington's disease cells. Soc. Neurosci. Abstr. 24: 970.
22. Zhang Y, Ona VO, Li M, Drozda M, Dubois-Dauphin M, Przedborski S, Ferrante RJ and Friedlander RM (2003) Sequential activation of individual caspases, and of alterations in Bcl-2 proapoptotic signals in a mouse model of Huntington's disease. J. Neurochem. 87: 1184–1192.
23. Kiechle T, Dedeoglu A, Kubilus J, Kowall NW, Beal MF, Friedlander RM, Hersch SM and Ferrante RJ (2002) Cytochrome *c*and caspase-9 expression in Huntington's disease. Neuromolecular Med. 1: 183–195.
24. Sugimoto M, Tahara H, Ide T and Furuichi Y (2004) Steps involved in immortalization and tumorigenesis in human B-lymphoblastoid cell lines transformed by Epstein–Barr virus. Cancer Res. 64: 3361–3364.
25. Fernando P, Kelly JF, Balazsi K, Slack RS and Megeney LA (2002) Caspase 3 activity is required for skeletal muscle differentiation. Proc. Natl. Acad. Sci. USA 99: 11025–11030.
26. Rigamonti D, Sipione S, Goffredo D, Zuccato C, Fossale E and Cattaneo E (2001) Huntingtin's neuroprotective activity occurs via inhibition of procaspase-9 processing. J. Biol. Chem. 276: 14545–14548.
27. Gervais FG, Singaraja R, Xanthoudakis S, Gutekunst CA, Leavitt BR, Metzler M, Hackam AS, Tam J, Vaillancourt JP, Houtzager V, Rasper DM, Roy S, Hayden MR and Nicholson DW (2002) Recruitment and activation of caspase-8 by the huntingtin-interacting protein Hip-1 and a novel partner Hippi. Nat. Cell Biol. 4: 95–105.
28. Ravikumar B, Vacher C, Berger Z, Davies JE, Luo S, Oroz LG, Scaravilli F, Baston DF, Duden R, O'Kane CJ and Rubinsztein DC (2004) Inhibition of mTOR induces autophagy and reduces toxicity of polyglutamine expansions in fly and mouse models of Huntington disease. Nat. Genet. 36: 585–595.
29. Nagata E, Sawa A, Ross CA and Snyder SH (2004) Autophagosome-like vacuole formation in Huntington's disease lymphoblasts. Neuroreport 15: 1325–1328.
30. Squitieri F, Cannella M, Sgarbi G, Maglione V, Falleni A, Lenzi P, Baracca A, Cislaghi G, Saft C, Ragona G, Russo MA, Thompson LM, Solaini G and Fomai F (2006) Severe ultrastructural mitochondrial changes in lymphoblasts homozygous for Huntington disease mutation. Mech Ageing Dev. 127: 217–220.
31. Seo H, Sonntag KC and Isacson O (2004) Generalized brain and skin proteasome inhibition in Huntington's disease. Ann. Neurol. 56: 319–328.
32. Metzler M, Helgason CD, Dragatsis I, Zhang T, Gan L, Pineault N, Zeitlin SO, Humphries RK and Hayden MR (2000) Huntingtin is required for normal hematopoiesis. Hum. Mol. Genet. 9: 387–394.
33. Kremer B, Almqvist E, Theilmann J, Spence N, Telenius H, Goldberg YP and Hayden MR (1995) Sex-dependent mechanisms for expansions and contractions of the CAG repeat on affected Huntington disease chromosomes. Am. J. Hum. Genet. 57: 343–350.
34. Cannella M, Simonelli M, D'Alessio C, Pierelli F, Ruggieri S and Squitieri F (2001) Presymptomatic tests in Huntington's disease and dominant ataxias. Neurol. Sci. 22: 55–56.
35. Blau HM and Webster C (1981) Isolation and characterization of human muscle cells. Proc. Natl. Acad. Sci. USA 78: 5623–5627.
36. Kaufman SJ and Foster RF (1988) Replicating myoblasts express a muscle-specific phenotype. Proc. Natl. Acad. Sci. USA 85: 9606–9610.
37. Authier FJ, Chazaud B, Plonquet A, Eliezer-Vanerot MC, Poron F, Belec L, Barlovatz-Meimon G and Gherardi RK (1999) Differential expression of the IL-1 system components during *in vitro* myogenesis: implication of IL-1beta in induction of myogenic cell apoptosis. Cell Death Differ. 6: 1012–1021.
38. Ly JD, Grubb DR and Lawen A (2003) The mitochondrial membrane potential ($\Delta\Psi_m$) in apoptosis; an update. Apoptosis 8: 115–128.
39. Pham NA, Robinson BH and Hedley DW (2000) Simultaneous detection of mitochondrial respiratory chain activity and reactive oxygen in digitonin-permeabilized cells using flow cytometry. Cytometry 41: 245–251.
40. Madesh M, Antonsson B, Srinivasula SM, Alnemri ES and Hajnoczky G (2002) Rapid kinetics of tBid-induced cytochrome *c* and Smac/DIABLO release and mitochondrial depolarization. J. Biol. Chem. 277: 5651–5659.

Supplementary Information accompanies the paper on Cell Death and Differentiation website (http://www.nature.com/cdd)